

# Spatially Resolved Conductivity of Rectangular Interconnects considering Surface Scattering - Part II: Circuit-Compatible Modeling

Xinkang Chen, and Sumeet Kumar Gupta, Senior *Member*, IEEE

**Abstract**— Interconnect conductivity modeling is a critical aspect for modern chip design. Surface scattering – an important scattering mechanism in scaled interconnects is usually captured using Fuchs-Sondheimer (FS) model which offers the average behavior of the interconnect. However, to support the modern interconnect structures (such as tapered geometries), modeling spatial dependency of conductivity becomes important. In Part I of this work, we presented a spatially resolved FS (SRFS) model for rectangular interconnects derived from the fundamental FS approach. While the proposed SRFS model offers both spatial-dependency of conductivity and its direct relationship with the physical parameters, its complex expression is not suitable for incorporation in circuit simulations. In this part, we build upon our SRFS model to propose a circuit-compatible conductivity model for rectangular interconnects accounting for 2D surface scattering. The proposed circuit-compatible model offers spatial resolution of conductivity as well as explicit dependence on the physical parameters such as electron mean free path ( $\lambda_0$ ), specularity ( $p$ ) and interconnect geometry. We validate our circuit-compatible model over a range of interconnect width/height (and  $\lambda_0$ ) and  $p$  values and show a close match with the physical SRFS model proposed in Part I (with error < 0.7%). We also compare our circuit-compatible model with a previous spatially resolved analytical model (appropriately modified for a fair comparison) and show that our model captures the spatial resolution of conductivity and the dependence on physical parameters more accurately. Finally, we present a semi-analytical equation for the average conductivity based on our circuit-compatible model.

**Index Terms**—Boltzmann transport equation, Fuchs-Sondheimer model, interconnect, 2D circuit-compatible conductivity model

## I. INTRODUCTION

The progression of technology scaling stands as a key driver for enhancing the electronic devices, facilitating improvements in speed, energy efficiency, and integration density. As we venture into sub-7nm technology nodes, numerous obstacles come to the forefront [1]. Among these, interconnects emerge as a formidable challenge which demands attention to sustain the scaling endeavor [2]. Various promising designs and materials for interconnects present potential solutions [3], [4], aiming to mitigate associated issues and enhance interconnect performance. Nonetheless, the scaling of interconnects remains a pivotal concern, validated by numerous studies predicting the interconnects as performance bottlenecks in advanced technology nodes due to multiple scaling challenges [1], [2].

Scaling the interconnect dimensions directly results in an increase in resistance, primarily due to a reduced cross-sectional area ( $A_W$ ). This phenomenon is not solely the result of reduction in the cross-sectional area over which conduction takes place but also stems from an increase in sidewall scattering yielding higher resistivity [5]. Both these factors significantly increase the resistance per unit length of the metal lines ( $r_{METAL} = \rho_W / A_W$ ) and via resistances ( $R_{VIA}$ ). To exacerbate matters, the active conduction area of the state-of-the-art copper (Cu)-based interconnects is typically smaller than their physical footprint. This limitation is attributed to the need for Cu to be enveloped within 1-2nm barrier layers (e.g. TaN) to mitigate electromigration [6], [7] and 1-2nm liners (e.g. Ta) for proper adhesion [6], [7]. Thus, to discern the scaling behavior of the interconnects (and explore possible solutions), understanding surface scattering is critical, for which modeling of surface scattering in interconnects becomes important.

In part I of this work, we discussed several modeling methods accounting for surface scattering and their limitations. The well-known Fuchs-Sondheimer (FS) theory [8] models surface scattering using fundamental physical equations. So far, the spatial dependence of conductivity using this approach has not been investigated. A recent empirical approach using “cosh” function to model the resistivity as a function of the location within the cross-section of the interconnect [9] provides a spatial-dependent resistivity model. This approach can be useful in modeling modern interconnect vias with a taper (i.e. wider openings at the top and narrower openings at the bottom

> REPLACE THIS LINE WITH YOUR MANUSCRIPT ID NUMBER (DOUBLE-CLICK HERE TO EDIT) <

$$\frac{\sigma_{SRFS}(x_n, y_n)}{\sigma_0} = \frac{3}{4} \int_{\theta=0}^{\pi} \eta(x_n, y_n, \theta) * \cos^2 \theta \sin \theta d\theta$$

$$\eta(x_n, y_n, \theta) = 2\pi - (1-p) \times \left[ 2 \int_{\Phi=0}^{\frac{\pi}{2}} \left( \frac{\left( e^{\frac{-\kappa_a}{2 \sin \theta \cos \Phi}} \times \cosh \left( \frac{\kappa_a \times x_n}{2 \sin \theta \cos \Phi} \right) \right)}{1 - p e^{\frac{-\kappa_a}{\sin \theta \cos \Phi}}} + \frac{\left( e^{\frac{-\kappa_b}{2 \sin \theta \sin \Phi}} \times \cosh \left( \frac{\kappa_b \times y_n}{2 \sin \theta \sin \Phi} \right) \right)}{1 - p e^{\frac{-\kappa_b}{\sin \theta \sin \Phi}}} \right) d\Phi \right. \\ \left. + \frac{1}{2} \sum_{n,d} \int_{\Phi=0}^{\frac{\pi}{2}} \left| \frac{e^{\frac{-\kappa_a \times d}{2 \sin \theta \cos \Phi}}}{1 - p e^{\frac{-\kappa_a}{\sin \theta \cos \Phi}}} - \frac{e^{\frac{-\kappa_b \times n}{2 \sin \theta \sin \Phi}}}{1 - p e^{\frac{-\kappa_b}{\sin \theta \sin \Phi}}} \right| d\Phi \right]$$

Where  $(n, d) \rightarrow \left\{ \begin{array}{l} (1 + y_n, 1 + x_n), (1 - y_n, 1 + x_n), \\ (1 + y_n, 1 - x_n), (1 - y_n, 1 - x_n) \end{array} \right\}$   $x_n = \frac{x}{a/2} \in [-1, 1], y_n \in \frac{y}{b/2} [-1, 1]; \quad \kappa_a = \frac{a}{\lambda_0}, \kappa_b = \frac{b}{\lambda_0}$  (1)

of the interconnects), as has been shown in [10]. However, the model, being empirical, lacks physical insights and relies on fitting parameters. In order to achieve both the spatial dependency and explicit relations to the physical parameters, we proposed a spatially resolved FS (SRFS) model derived from the Boltzmann transport equation (BTE) in Part I of this paper. However, like the FS model, SRFS model involves computation of complex integrals, which makes it unsuitable for integrating in computer-aided-design (CAD) software or circuit simulators. Thus, a circuit-compatible model for conductivity accounting for surface scattering is needed, which offers spatial resolution and direction relationships to the interconnect material/geometric parameters.

In this part of our paper, we address this need by building upon the SRFS model of Part I and proposing circuit-compatible 2D conductivity model for rectangular interconnects. The proposed approach models the conductivity (accounting for surface scattering) as a function of the location within the cross-section as well as physical parameters such as electron mean free path, specularity and interconnect width/height. The main contributions of Part II of this work are summarized as follows:

- We present a circuit-compatible model for spatially resolved conductivity of rectangular interconnects based on the SRFS model developed in part I. We refer to our model as “SRFS-based Circuit-Compatible Conductivity” model or SRFS-C3 model.
- We propose well-behaved functions for the parameters of the SRFS-C3 model relating them to the electron mean free path ( $\lambda_0$ ) and specularity of sidewall scattering ( $p$ ).
- We extensively validate our circuit-compatible model with the SRFS model showing an excellent match with respect to the spatial profile as well as trends with varying interconnect width/height,  $\lambda_0$  and  $p$ .
- We compare the proposed SRFS-C3 model with the previously proposed “cosh” model [9] (appropriately modified for fair comparison) highlighting the advantages of the proposed model.
- We present a continuous semi-analytical formula for obtaining the average conductivity and validate it against previous FS-based models.

## II. BACKGROUND

### A. Spatially Resolved FS (SRFS) Model

In Part I of this work, we proposed a spatially resolved FS (SRFS) model derived from the basic Boltzmann transport equation. The main advantage of the SRFS model is that conductivity is expressed as a function of the location within the interconnect cross-section, and it retains the explicit relationships of conductivity to fundamental electron transport parameters such as electron mean free path, conductor dimensions, and specularity (as in the original FS model). The full expression is shown in (1). This expression is for a rectangular conductor with width  $a$  and height  $b$  with the origin at the center of the wire. Thus, the wire cross sectional width is from  $x = -a/2$  to  $+a/2$  and its height is from  $y = -b/2$  to  $+b/2$ . We define  $\kappa_a = \frac{a}{\lambda_0}$  and  $\kappa_b = \frac{b}{\lambda_0}$  [11] and normalize the spatial coordinates as  $x_n = x/(a/2)$  and  $y_n = y/(b/2)$  in this model. As can be observed, the conductivity is a function of  $x_n$  and  $y_n$ , the bulk copper conductivity ( $\sigma_0$ ), specularity ( $p$ , where  $0 < p < 1$  and  $p = 0$  for diffusive and  $p = 1$  for completely elastic scattering) and the parameters  $\kappa_a$  and  $\kappa_b$  (which capture the interconnect width/height and the electron mean free path).

The SRFS model contains nested integrals, thus its evaluation requires a considerable amount of computing resources. To use a conductivity model on CAD software and circuit simulators, the computing requirements of the SRFS model need to be reduced, while retaining its physical insights and spatial resolution. The proposed circuit-compatible model aims to meet these requirements, as will be discussed subsequently.

### B. The “cosh” Model with Spatial Dependency

A semi-empirical resistivity model proposed by [9] can capture the impact of surface scattering from the four barrier interfaces, based on the conductor’s dimensions and location within the cross-section.

$$\rho(x, y) = \rho_0 + \rho_q \left( \frac{\cosh\left[\frac{x}{\lambda_q}\right]}{\cosh\left[\frac{a}{2\lambda_q}\right]} + \frac{\cosh\left[\frac{y}{\lambda_q}\right]}{\cosh\left[\frac{b}{2\lambda_q}\right]} \right) \quad (2)$$

Here,  $\rho_0$  lumps bulk resistivity and other scattering mechanisms (such as grain boundary scattering) and the rest of it accounting for spatial dependence of resistivity due to surface scattering, with  $\rho_q$  and  $\lambda_q$  as the model fitting parameters. The

> REPLACE THIS LINE WITH YOUR MANUSCRIPT ID NUMBER (DOUBLE-CLICK HERE TO EDIT) <

conductivity can be obtained by integrating the reciprocal of (2) over the Cu conductor's cross section. The analysis in [9] shows a good match of the average conductivity with the experiments. The main advantage of this approach (referred to as the ‘‘cosh’’ model subsequently) is its spatial resolution of resistivity. However, this method does not directly capture the relationship of the conductivity with the physical parameters (such as  $p$ ,  $\lambda_0$  etc.). We have also shown in Part I that the spatial profile predicted by this empirical approach (based on the parameters in [9]) is quite different compared to the physical SRFS model (derived from fundamental equations), even though the average conductivity value for the two models is the same (and matched to the experiments in [9]). However, the question is if the ‘‘cosh’’ approach can be used in conjunction with the SRFS model for better estimates of the model fitting parameters and hence, better prediction of the spatial profile of the conductivity. We explore this later in the paper to establish the baseline for the proposed circuit-compatible model.

### III. SPATIALLY RESOLVED FS-BASED CIRCUIT-COMPATIBLE CONDUCTIVITY (SRFS-C3) MODEL

As noted before, the SRFS model proposed in Part I provides spatial resolution as well the connections to the physical parameters but lacks circuit compatibility. In other words, if the conductivity at every point in the cross-section of the interconnect is calculated using the SRFS model, the time of computation would be prohibitively large for a circuit or CAD simulation. To get around this problem, the basic premise of our SRFS-C3 model is to develop an analytical function which can predict the spatial profile of the conductivity based on the conductivity values obtained from the SRFS model for only a few spatial locations. As we will show later, the SRFS-C3 approach requires the SRFS conductivity values ( $\sigma_{SRFS}$ ) from (1) for only 4 points for a rectangular interconnect (and only 3 points for a symmetric square interconnect). Thus, by calling the SRFS model only four times and using the proposed analytical function, the spatial profile for the entire cross-section as well as the trends with respect to varying  $p$ ,  $\lambda_0$ ,  $a$  and  $b$  can be predicted by the SRFS-C3 with a good accuracy. This helps in significantly speeding the computation, thus making the SRFS-C3 model circuit compatible. To explain our technique, let us first start with the 1D SRFS-C3 model for the spatially-resolved conductivity. We will then extend it to 2D.

#### A. 1D SRFS-C3 Model

While analyzing the SRFS model using (1), we observe that the partial derivative of the spatially-resolved conductivity ( $\sigma$ ) with respect to  $x$  (or  $y$ ) has a profile similar to the  $\tanh^{-1}$  function (especially near the center of the interconnect). However, if we integrate the  $\tanh^{-1}$  function to find the conductivity, the resultant model is unable to predict the sharp slopes closer to the edges of the interconnect, especially for high values of  $\kappa_a$ . On the other hand, the cosh function used in [9] tracks the sharpness of the spatial profile near the edges for a wide range of  $\kappa_a$ , but is unable to match the overall space dependence (as also shown in Part I). Therefore, we proceed by combining the  $\tanh^{-1}$  and cosh functions as follows. We start with the second partial derivative of  $\sigma$  with respect to  $x_n$  to reflect the functional attributes of  $\tanh^{-1}$  based conductivity derivative combined with

cosh-based conductivity profile. For that, we use the following analytical function.

$$\frac{\partial^2 \sigma}{\partial x_n^2} = \frac{\alpha_x \cosh(\beta_a x_n)}{1 - x_n^2} \quad (3)$$

Here, cosh function is used to represent the double derivative of cosh-based conductivity profile and  $\frac{1}{1-x_n^2}$  is used to represent the derivative of  $\tanh$ -based conductivity derivative. The two are multiplied to combine the attributes of the respective functions. The parameters  $\alpha_x$  and  $\beta_a$  will be discussed in detail subsequently.

To calculate the conductivity, we perform a double integral of (3) with respect to  $x_n$ , use the boundary conditions at  $x_n=0$  (center of the wire) and  $x_n=1$  (edge of the wire) and obtain

$$\sigma(x_n) = \sigma|_{x_n=0} - (\sigma|_{x_n=0} - \sigma|_{x_n=1}) \times \frac{\xi(x_n, \beta_a)}{\xi_1(\beta_a)} \quad (4)$$

where

$$\begin{aligned} \xi(x_n, \beta_a) = & (1 + x_n) \{ \cosh(\beta_a) [ \text{Chi}(\beta_a(1 + x_n)) ] \\ & - \sinh(\beta_a) [ \text{Shi}(\beta_a(1 + x_n)) ] \} \\ & + (1 - x_n) \{ \cosh(\beta_a) [ \text{Chi}(\beta_a(1 - x_n)) ] \\ & - \sinh(\beta_a) [ \text{Shi}(\beta_a(1 - x_n)) ] \} \end{aligned} \quad (5)$$

and

$$\begin{aligned} \xi_1(\beta_a) = & \xi(1, \beta_a) \\ = & 2 \times [ \cosh(\beta_a) (\text{Chi}(2\beta_a) - \text{Chi}(\beta_a)) \\ & - \sinh(\beta_a) (\text{Shi}(2\beta_a) - \text{Shi}(\beta_a)) ] \end{aligned} \quad (6)$$

Here,  $\text{Chi}$  is the cosh-integral (‘coshint’ in MATLAB) and  $\text{Shi}$  is the sinh-integral (‘sinhint’ in MATLAB) functions. The parameter  $\beta_a$  is used for fitting and is obtained by minimizing the mean square error (MSE) between the circuit-compatible and the SRFS model.  $\beta_a$  is a function of  $\kappa_a$  (and therefore,  $a$  and  $\lambda_0$ ) and  $p$ . We will discuss the  $\beta_a$  fitting and an analytical model for  $\beta_a$  in detail later. The parameter  $\alpha_x$  is assimilated in the expressions above once the boundary conditions are applied. The boundary values  $\sigma|_{x_n=0}$  and  $\sigma|_{x_n=1}$  need to be obtained from the 1D SRFS model i.e. using (1) with  $y_n$ -dependent terms ignored (e.g. by setting  $\kappa_b \rightarrow \infty$ , see Part I for details). Note, since the spatial profile is expected to be symmetric with respect to the origin,  $\sigma|_{x_n=1} = \sigma|_{x_n=-1}$ , and therefore, we use the boundary conditions at the center and edge of the wire along the  $x$  direction. Thus, by using just 2 values from the 1D SRFS model, the proposed 1D SRFS-C3 model in (4) can predict the spatial profile for any  $x_n$  (in the range of -1 and 1). We can repeat the same procedure for obtaining the spatial dependence with respect to  $y_n$  with its own fitting parameter  $\beta_b$  (function of  $p$  and  $\kappa_b$  (and hence,  $b$  and  $\lambda_0$ )) and boundary points  $\sigma|_{y_n=0}$  and  $\sigma|_{y_n=1}$  obtained from the SRFS model.

With this discussion, let us now explain the 2D SRFS-C3 model.

#### B. 2D SRFS-C3 Model

To obtain the 2D SRFS-C3 model from the 1D model of (4), we use the following procedure.

- Given an arbitrary location  $(x_n, y_n)$  within the cross-section of the interconnect (where both  $x_n$  and  $y_n$  range from -1 to 1)

> REPLACE THIS LINE WITH YOUR MANUSCRIPT ID NUMBER (DOUBLE-CLICK HERE TO EDIT) <

at which we want to find  $\sigma(x_n, y_n)$ , we first use (4) to obtain  $\sigma(x_n, 0)$  as

$$\sigma(x_n, 0) = \sigma_{SRFS}(0,0) - (\sigma_{SRFS}(0,0) - \sigma_{SRFS}(1,0)) \times \frac{\xi(x_n, \beta_a)}{\xi_1(\beta_a)} \quad (7)$$

Here,  $\sigma_{SRFS}$  refers to the SRFS model derived in part I and given by (1).

- Following a similar process, we obtain  $\sigma(x_n, 1)$  as

$$\sigma(x_n, 1) = \sigma_{SRFS}(0,1) - (\sigma_{SRFS}(0,1) - \sigma_{SRFS}(1,1)) \times \frac{\xi(x_n, \beta_a)}{\xi_1(\beta_a)} \quad (8)$$

- Then, we use the 1D equation along  $y$  to calculate  $\sigma(x_n, y_n)$  as

$$\sigma(x_n, y_n) = \sigma(x_n, 0) - (\sigma(x_n, 0) - \sigma(x_n, 1)) \times \frac{\xi(y_n, \beta_b)}{\xi_1(\beta_b)} \quad (9)$$

Here,  $\sigma(x_n, 0)$  and  $\sigma(x_n, 1)$  are obtained from (7) and (8).

Thus, we can calculate the conductivity at any point within the cross-section of the interconnect. We follow the process described above to obtain an analytical formula for  $\sigma(x_n, y_n)$

$$\begin{aligned} \sigma(x_n, y_n) = & \sigma_{SRFS}(0,0) \\ & - (\sigma_{SRFS}(0,0) - \sigma_{SRFS}(1,0)) \times \frac{\xi(x_n, \beta_a)}{\xi_1(\beta_a)} \\ & - (\sigma_{SRFS}(0,0) - \sigma_{SRFS}(0,1)) \times \frac{\xi(y_n, \beta_b)}{\xi_1(\beta_b)} \\ & - (\sigma_{SRFS}(0,1) + \sigma_{SRFS}(1,0) - \sigma_{SRFS}(0,0) - \sigma_{SRFS}(1,1)) \\ & \times \frac{\xi(x_n, \beta_a)}{\xi_1(\beta_a)} \frac{\xi(y_n, \beta_b)}{\xi_1(\beta_b)} \end{aligned} \quad (10)$$

It can be noted that we need only four points from the SRFS model of (1) to compute the entire spatial profile. This is made possible by the analytical  $\xi$  function described by (5), which forms the basis of the proposed SRFS-C3 model. It is also noteworthy that (10) comprises of terms with sole dependences on  $x_n$  (2<sup>nd</sup> term) or  $y_n$  (3<sup>rd</sup> term), but additionally it also captures the cross interactions through the last term which has the product of  $x_n$  and  $y_n$ -dependent terms. This is similar to the SRFS model in equation (1) which has sole  $x_n$  and  $y_n$ -dependent terms and a term which depends on both  $x_n$  and  $y_n$ .

#### D. SRFS-C3 Parameter $\beta_a(\beta_b)$ : Fitting and Modeling

The parameter  $\beta_a(\beta_b)$  can be obtained by minimizing the mean square error (MSE) between the SRFS-C3 and SRFS models. To keep the model simple, we perform the fitting independently for  $\beta_a$  and  $\beta_b$  (that is neglecting the cross interaction between  $x_n$  and  $y_n$ ). As noted before,  $\beta_a(\beta_b)$  is a function of  $\kappa_a(\kappa_b)$  and  $p$ . Hence, we find the best fit for  $\beta_a$  by sweeping  $\kappa_a$  and  $p$ . (Note, by relating  $\beta_a$  to  $\kappa_a$ , we can seamlessly find  $\beta_b$  by substituting  $\kappa_b$  for  $\kappa_a$ . Henceforth, we will present our discussions in terms of  $\beta_a$  and  $\kappa_a$ ). The best fit values for  $\beta_a$  for different  $\kappa_a$  and  $p$  shown in Fig. 1. Interestingly, for  $\kappa_a > 1$ ,  $\beta_a$  is independent of  $p$  and exhibits a linear behavior with respect to  $\kappa_a$  with a slope of  $\frac{2}{\pi}$ . On the other hand, for small  $\kappa_a$  ( $\kappa_a < 1$ ),  $\beta_a$  shows a deviation from this linear behavior and also shows a dependence on  $p$ . Further, at  $p=0$  and  $\kappa_a \rightarrow 0$ ,  $\beta_a \rightarrow 1$ .

The relationship of  $\beta_a$  with  $\kappa_a$  and  $p$  can be approximately captured using the following equation:

$$\beta_a = \frac{2}{\pi} \kappa_a + \tanh\left(\frac{\kappa_a}{\epsilon p}\right) \quad (11)$$

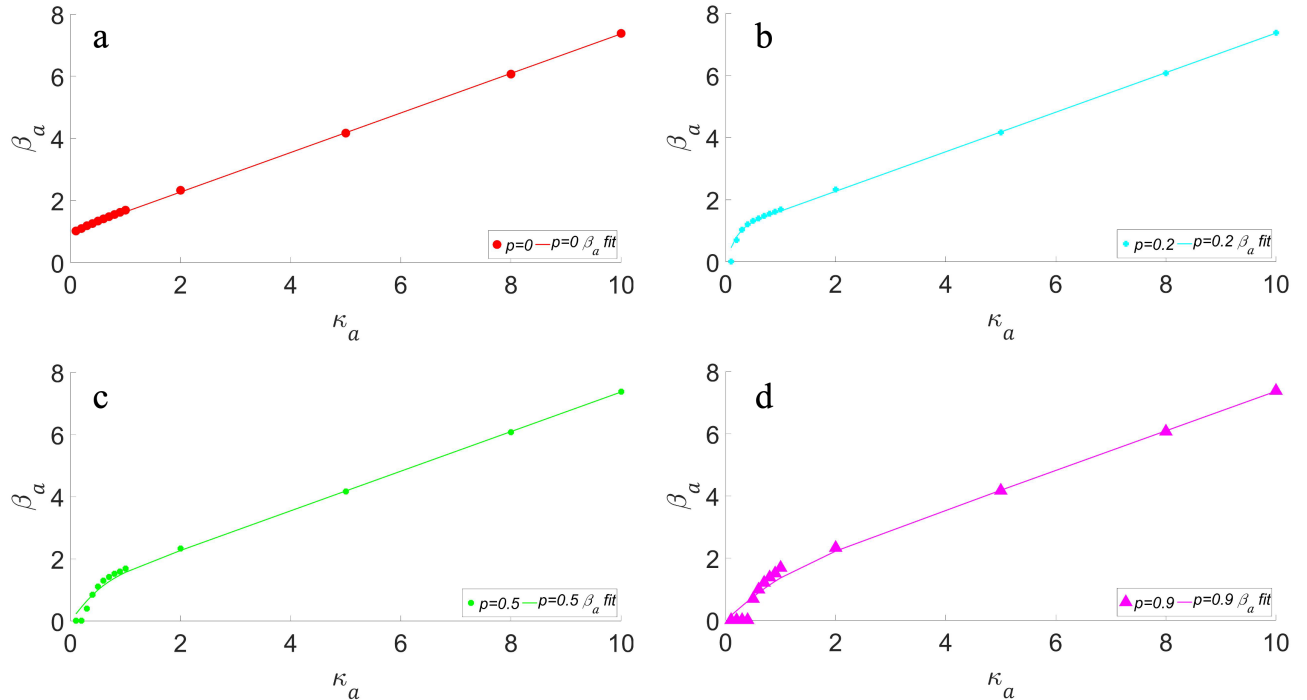


Fig. 1.  $\beta_a$  vs  $\kappa_a$  showing the best fit in dots and model approximate fit obtain from (11) in lines for a)  $p=0$  b)  $p=0.2$  c)  $p=0.5$  d)  $p=0.9$

> REPLACE THIS LINE WITH YOUR MANUSCRIPT ID NUMBER (DOUBLE-CLICK HERE TO EDIT) <

Final SRFS-C3 model for conductivity accounting for specular surface scattering

$$\sigma_{SRFS-C3}(x_n, y_n) = \sigma_{SRFS}(0,0) - (\sigma_{SRFS}(0,0) - \sigma_{SRFS}(1,0)) \times \frac{\xi(x_n, \beta_a)}{\xi_1(\beta_a)} - (\sigma_{SRFS}(0,0) - \sigma_{SRFS}(0,1)) \times \frac{\xi(y_n, \beta_b)}{\xi_1(\beta_b)} - (\sigma_{SRFS}(0,1) + \sigma_{SRFS}(1,0) - \sigma_{SRFS}(0,0) - \sigma_{SRFS}(1,1)) \times \frac{\xi(x_n, \beta_a)}{\xi_1(\beta_a)} \frac{\xi(y_n, \beta_b)}{\xi_1(\beta_b)}$$

where

$$\begin{aligned} \xi(x_n, \beta_a) &= (1 + x_n) \{ \cosh(\beta_a) [Chi(\beta_a(1 + x_n))] - \sinh(\beta_a) [Shi(\beta_a(1 + x_n))] \} \\ &\quad + (1 - x_n) \{ \cosh(\beta_a) [Chi(\beta_a(1 - x_n))] - \sinh(\beta_a) [Shi(\beta_a(1 - x_n))] \} \\ \xi(y_n, \beta_b) &= (1 + y_n) \{ \cosh(\beta_b) [Chi(\beta_b(1 + y_n))] - \sinh(\beta_b) [Shi(\beta_b(1 + y_n))] \} \\ &\quad + (1 - y_n) \{ \cosh(\beta_b) [Chi(\beta_b(1 - y_n))] - \sinh(\beta_b) [Shi(\beta_b(1 - y_n))] \} \end{aligned}$$

and

$$\begin{aligned} \xi_1(\beta_a) &= 2 \times [ \cosh(\beta_a) (Chi(2\beta_a) - Chi(\beta_a)) - \sinh(\beta_a) (Shi(2\beta_a) - Shi(\beta_a)) ] \\ \xi_1(\beta_b) &= 2 \times [ \cosh(\beta_b) (Chi(2\beta_b) - Chi(\beta_b)) - \sinh(\beta_b) (Shi(2\beta_b) - Shi(\beta_b)) ] \end{aligned}$$

$$x_n = \frac{x}{a/2} \in [-1, 1], \quad y_n \in \frac{y}{b/2} [-1, 1]; \quad \kappa_a = \frac{a}{\lambda_0}, \quad \kappa_b = \frac{b}{\lambda_0}$$

$$\beta_a = \frac{2}{\pi} \kappa_a + \tanh\left(\frac{\kappa_a}{1.2p}\right), \quad \beta_b = \frac{2}{\pi} \kappa_b + \tanh\left(\frac{\kappa_b}{1.2p}\right) \quad (12)$$

Here,  $\varepsilon$  is a fitting parameter and is found to be equal to 1.2 by minimizing the MSE between (11) and the best fit values of  $\beta_a$ . Fig. 1a-d illustrates the behavior of (11) for different  $p$  and  $\kappa$  values, demonstrating that (11) can model the relationship between  $\beta_a$ ,  $\kappa_a$  and  $p$  with reasonable accuracy using a simple equation (except for some deviations for small  $\kappa_a$ ).

The complete SRFS-C3 model is summarized at the top of next page. Notice that the SRFS-C3 expression is based on conductivity subtraction which is more physical as we noted in Part I compared to resistivity addition used in the ‘‘cosh’’ model.

The SRFS-C3 model is general and can also be applied to thin films (of thickness  $b$  along the  $y$ -direction). For that, we set  $\kappa_a \rightarrow \infty$  and obtain

$$\begin{aligned} \sigma_{SRFS-C3}(y_n) &= \sigma_{SRFS}(0,0) \\ &\quad - (\sigma_{SRFS}(0,0) - \sigma_{SRFS}(0,1)) \times \frac{\xi(y_n, \beta_b)}{\xi_1(\beta_b)} \end{aligned}$$

Before we discuss the comparison of the SRFS-C3 with the SRFS model, we will first explore the question: Can the ‘‘cosh’’ model (similar to [9]) be used in conjunction with only a few values obtained from the SRFS model (similar to our approach) to predict spatial profile of the conductivity.

#### IV. MODIFIED ‘‘COSH’’ MODEL

In Part I of this work, we compared our proposed SRFS conductivity model and the ‘‘cosh’’ model from [9] by matching their average conductivity. We observe significant differences in their spatial profiles. In this section, we use the ‘‘cosh’’ model in conjunction with the SRFS model, following a similar approach as the SRFS-C3 model. In the next section, we will

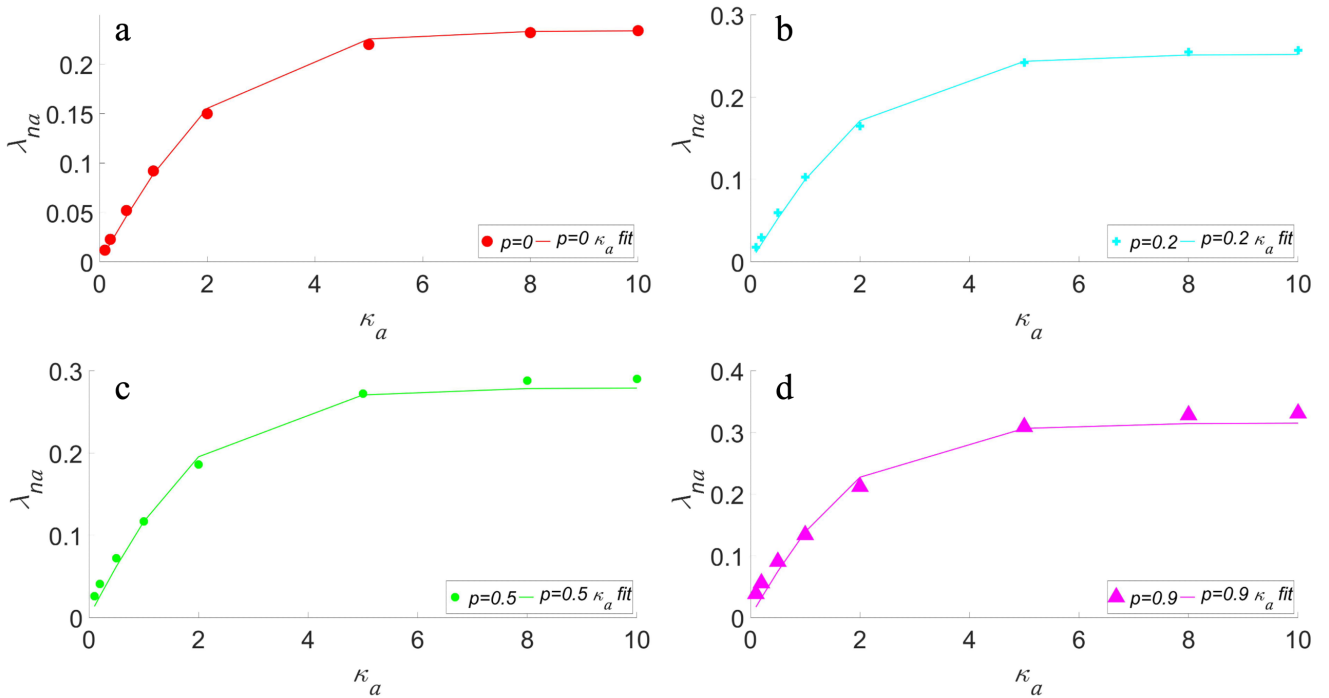


Fig. 2.  $\lambda_n$  vs  $\kappa_a$  showing the best fit in dots and model approximate fit obtain from (14) in lines for a)  $p=0$  b)  $p=0.2$  c)  $p=0.5$  d)  $p=0.9$

> REPLACE THIS LINE WITH YOUR MANUSCRIPT ID NUMBER (DOUBLE-CLICK HERE TO EDIT) <

$$\rho(x_n, y_n) = \rho_b + \rho_{qx} \left( \frac{\cosh \left[ \frac{\kappa_a x_n}{2\lambda_{na}} \right] - 1}{\cosh \left[ \frac{\kappa_a}{2\lambda_{na}} \right] - 1} \right) + \rho_{qy} \left( \frac{\cosh \left[ \frac{\kappa_b y_n}{2\lambda_{nb}} \right] - 1}{\cosh \left[ \frac{\kappa_b}{2\lambda_{nb}} \right] - 1} \right) - \rho_q \left( \frac{\cosh \left[ \frac{\kappa_a x_n}{2\lambda_{na}} \right] - 1}{\cosh \left[ \frac{\kappa_a}{2\lambda_{na}} \right] - 1} \right) \times \left( \frac{\cosh \left[ \frac{\kappa_b y_n}{2\lambda_{nb}} \right] - 1}{\cosh \left[ \frac{\kappa_b}{2\lambda_{nb}} \right] - 1} \right)$$

$$\rho_b = \frac{1}{\sigma_{SRFS}(0,0)} \quad \rho_{qx} = \frac{1}{\sigma_{SRFS}(1,0)} - \rho_b \quad \rho_{qy} = \frac{1}{\sigma_{SRFS}(0,1)} - \rho_b$$

$$\rho_q = \frac{1}{\sigma_{SRFS}(1,0)} + \frac{1}{\sigma_{SRFS}(0,1)} - \frac{1}{\sigma_{SRFS}(0,0)} - \frac{1}{\sigma_{SRFS}(1,1)}$$
(13)

compare the proposed SRFS-C3 model the modified ‘‘cosh’’ model and how well they match the physical SRFS model.

We utilize the ‘‘cosh’’ model as the analytical function to predict the spatial profile of conductivity based on a few conductivity values obtained from the SRFS model i.e. equation (1). Following the similar approach as the last sub-section, we find four values from the SRFS model -  $\sigma_{SRFS}(0,0)$ ,  $\sigma_{SRFS}(1,0)$ ,  $\sigma_{SRFS}(0,1)$  and  $\sigma_{SRFS}(1,1)$ . The modified normalized ‘‘cosh’’ model is presented in (13),

Here  $\lambda_{na}(= \lambda_{qa}/\lambda_0)$  and  $\lambda_{nb}(= \lambda_{qb}/\lambda_0)$  are the new model fitting parameters (recall,  $\lambda_q$  is the fitting parameter in (2) from [9]). We find the best fitting value for  $\lambda_{na}(\lambda_{nb})$  based on minimizing the MSE with respect to the SRFS model.

The relationship between  $\lambda_{na}$  and  $\kappa_a$  (and hence,  $\lambda_{nb}$  and  $\kappa_b$ ) for different  $p$  values is illustrated in Fig. 2a-d. We proposed an approximate fitting expression as follows:

$$\lambda_{na} = 0.234 * \tanh(0.4\kappa_a) + 0.0875 * (\tanh(0.7\kappa_a) + 0.03) * p \quad (14)$$

The fitting expression results for different  $p$  and  $\kappa_a$  values are presented in Fig. 2a-d. The  $\lambda_{na}$  fitting expression in (14) is a bit more complex compared to  $\beta_a$  of (11) used in the proposed SRFS-C3 model. Moreover, the accuracy of the fit for (14) is also not as good as (11). Also, as we have pointed out before in section III, the modified ‘‘cosh’’ model is based on resistivity addition. In contrast, the proposed SRFS-C3 is based on conductivity subtraction, which is more consistent with the physical models of the original FS [8] and our SRFS approach.

## V. ANALYSIS OF THE SPATIAL PROFILE OF CONDUCTIVITY

In this section, we compare the spatial resolution of conductivity of a square interconnect ( $\kappa_a = \kappa_b = \kappa$ ) predicted by the proposed SRFS-C3 model, the modified ‘‘cosh’’ model and the accurate physical SRFS model for six  $\kappa$  values (0.2, 0.5, 1, 2, 5 and 10) with three  $p$  values (0, 0.5 and 0.9), covering a wide range of these parameters. (We have made similar comparisons for rectangular wires with similar conclusions; here, we do not include the results to avoid repetition). We first show the comparison using the best fitting (refer as B/F) values of  $\beta_a$  and  $\lambda_{na}$  for the SRFS-C3 and modified ‘‘cosh’’ models, respectively (i.e. without using the approximate models given by (11) and (14)). This will provide the comparison between the best versions of the models. Then, we show the comparison with approximate models for the fitting parameters (11) and (14) incorporated (refer as F).

The comparisons for the best fitting values of  $\beta_a$  and  $\lambda_{na}$  are shown in Fig. 3. We show the profile with respect to  $x_n$  for  $y_n = 0$  and  $y_n = 0.9$ . It can be observed that the SRFS-C3 model offers an excellent match to the physical SRFS model across a wide range of  $\kappa_a$  and  $p$ . Furthermore, compared to the modified

‘‘cosh’’ model, the proposed SRFS-C3 exhibits a better match with the SRFS model. The only exception is at very small  $\kappa_a$  and high  $p$  where the modified ‘‘cosh’’ performs *slightly* better.

For  $y_n = 0.9$ , the limitations of the modified ‘‘cosh’’ model become even more evident. On the other hand, the SRFS-C3 model shows a close match to the SRFS for both  $y_n = 0$  and 0.9. We also report the error averaged across the whole interconnect cross section between the SRFS-C3 and SRFS, and modified ‘‘cosh’’ and SRFS models for best fit in Table I and approximate fit cases in Table II. Maximum error averaged across the whole interconnect cross section in Table III and Table IV correspondingly. For the best fit case, it can be observed that the average error for SRFS-C3 is  $< 0.4\%$  across all  $\kappa$  and  $p$ , and the maximum error is  $< 6\%$ . On the other hand, for modified ‘‘cosh’’, the average error  $< 3.5\%$ , and the maximum error is  $< 23.1\%$ .

TABLE I

Average error between SRFS-C3 and SRFS and modified ‘‘cosh’’ and SRFS model (best fit)

		SRFS-C3						Modified ‘‘cosh’’					
$\kappa$	$p$	0.2		0.5		1		2		5		10	
		0	0.2%	1.4%	0.2%	1.8%	0.3%	2.4%	0.4%	3.2%	0.3%	3.5%	0.3%
0.5	0.1%	0.1%	0.0%	0.3%	0.0%	0.5%	0.1%	0.9%	0.1%	1.2%	0.1%	0.9%	
0.9	0.1%	0.0%	0.0%	0.1%	0.0%	0.2%	0.1%	0.5%	0.3%	0.8%	0.3%	0.8%	

TABLE II

Average error between SRFS-C3 and SRFS and modified ‘‘cosh’’ and SRFS model (approximate fit)

		SRFS-C3						Modified ‘‘cosh’’					
$\kappa$	$p$	0.2		0.5		1		2		5		10	
		0	0.2%	2.8%	0.3%	2.3%	0.5%	2.4%	0.7%	3.2%	0.3%	3.5%	0.3%
0.5	0.2%	0.8%	0.1%	0.6%	0.2%	0.6%	0.2%	0.9%	0.1%	1.2%	0.1%	0.9%	
0.9	0.0%	0.1%	0.0%	0.1%	0.1%	0.1%	0.1%	0.1%	0.0%	0.2%	0.0%	0.2%	

TABLE III

Maximum error between SRFS-C3 and SRFS and modified ‘‘cosh’’ and SRFS model (best fit)

		SRFS-C3						Modified ‘‘cosh’’					
$\kappa$	$p$	0.2		0.5		1		2		5		10	
		0	0.9%	5.5%	1.2%	7.7%	1.8%	10.0%	3.0%	15.9%	5.1%	22.0%	6.0%
0.5	0.3%	0.3%	0.1%	1.0%	0.2%	1.8%	0.8%	3.3%	1.6%	5.4%	2.0%	5.9%	
0.9	0.1%	0.0%	0.0%	0.1%	0.0%	0.2%	0.1%	0.5%	0.3%	0.8%	0.3%	0.8%	

TABLE IV

Maximum error between SRFS-C3 and SRFS and modified ‘‘cosh’’ and SRFS model (approximate fit)

		SRFS-C3						Modified ‘‘cosh’’					
$\kappa$	$p$	0.2		0.5		1		2		5		10	
		0	0.9%	6.4%	1.4%	5.8%	2.3%	10.0%	3.6%	16.7%	5.0%	22.6%	6.1%
0.5	0.4%	1.5%	0.2%	1.3%	0.5%	1.8%	1.0%	3.7%	1.6%	5.4%	2.0%	5.9%	
0.9	0.1%	0.1%	0.0%	0.2%	0.1%	0.2%	0.2%	0.6%	0.3%	0.8%	0.3%	0.8%	

&gt; REPLACE THIS LINE WITH YOUR MANUSCRIPT ID NUMBER (DOUBLE-CLICK HERE TO EDIT) &lt;

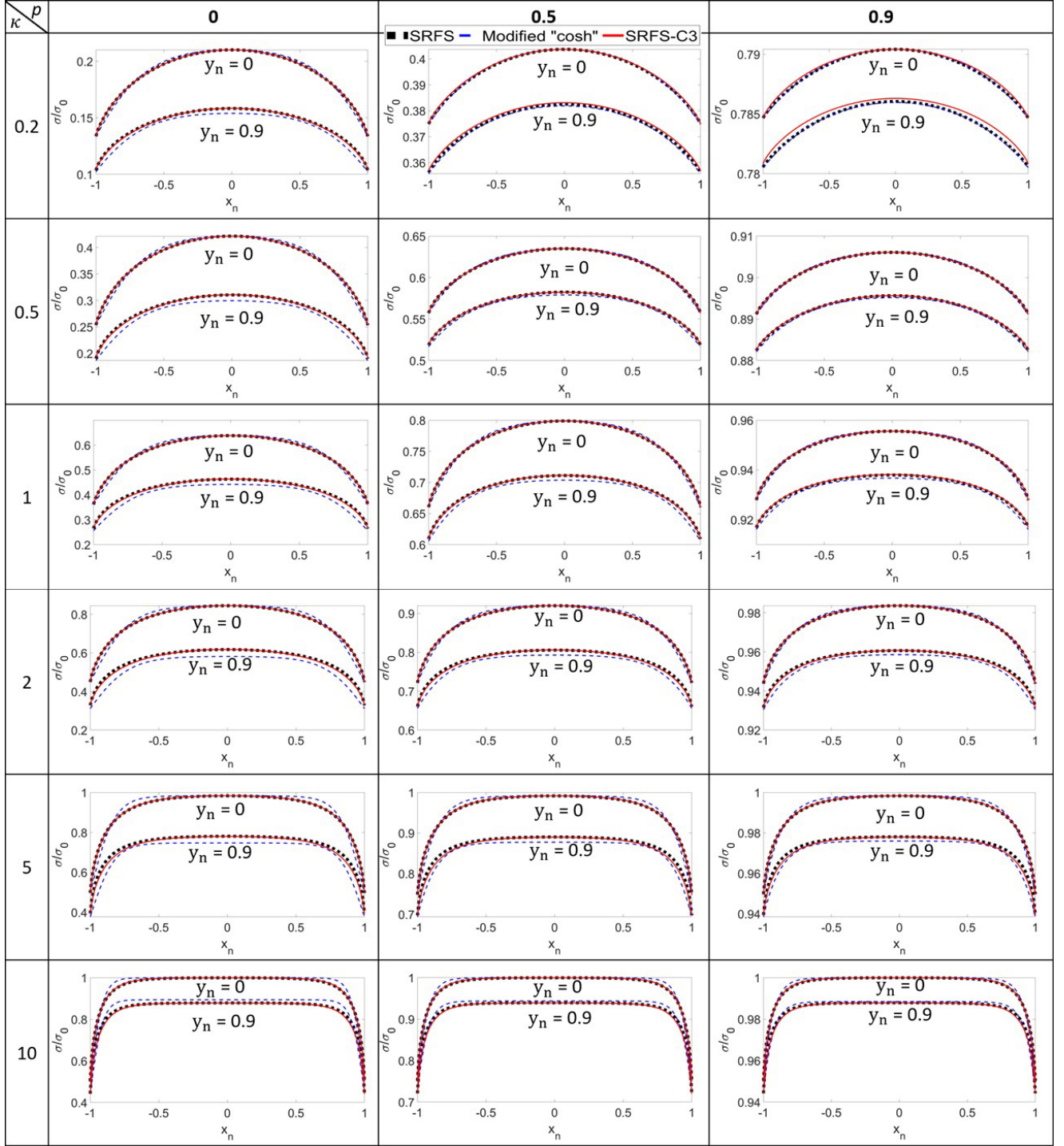


Fig. 3. The spatial profiles for  $\sigma/\sigma_0$  (conductivity normalized to bulk conductivity) versus  $x_n$  ( $x_n=x/(a/2)$ ) for  $y_n$  ( $y_n=y/(b/2)$ ) = 0, 0.9 for different  $\kappa$  and  $p$ . The model parameters correspond to the best fitting scenario.

Let us now look at the comparisons in Fig 4 in which we use the approximate models for  $\beta_a$  and  $\lambda_{na}$ . Like before, the proposed SRFS-C3 model exhibits an excellent match with the SRFS model across the entire range of  $\kappa$  and  $p$  considered. Also, it performs much better than the modified “cosh” model. From Table III and IV, it can be observed that the average error for SRFS-C3 is  $< 0.7\%$  across all  $\kappa$  and  $p$ , and the maximum error is  $< 6.1\%$ . On the other hand, for modified “cosh”, the average error  $< 3.5\%$ , and the maximum error is  $< 23\%$ . The proposed SRFS-C3 model has considerable less error for all range of

dimensions and specularity compared to modified “cosh” model.

## VI. ANALYTICAL AVERAGE CONDUCTIVITY MODEL DERIVED FROM SRFS-C3 MODEL

A remarkable implication of the SRFS-C3 model is that it can yield a continuous analytical model for the average conductivity accounting for surface scattering in rectangular interconnects for a wide range of the physical parameters. As

> REPLACE THIS LINE WITH YOUR MANUSCRIPT ID NUMBER (DOUBLE-CLICK HERE TO EDIT) <

we noted from Part I that in [12], the FS model for square wires ( $\kappa_a = \kappa_b$ ) for  $p=0$  was approximated to provide different analytical expressions for different regimes (such as for  $\kappa_a \gg 1$ ,  $\kappa_a > 4$ ,  $\kappa_a \ll 1$ ,  $\kappa_a \sim 1$  etc.). While highly useful in providing compact models for average conductivity and relating them to physical parameters, these expressions do not cover the entire range of  $\kappa_a$ . Some follow-up works have extended these expressions for rectangular wires and for

general  $p$ , but the limitations of these expressions in terms of their validity for only a certain range of  $\kappa_a$  still remain. With the SRFS-C3 model, we get the following benefits: (1) A single model is valid for a wide range of  $\kappa_a$ ,  $\kappa_b$  and  $p$ . (2) The model is analytical and readily integrable and (3) The model shows a close match with the physical SRFS model. Hence, we can integrate the SRFS-C3 model to get the average conductivity. In other words, we can get around the limitations of the

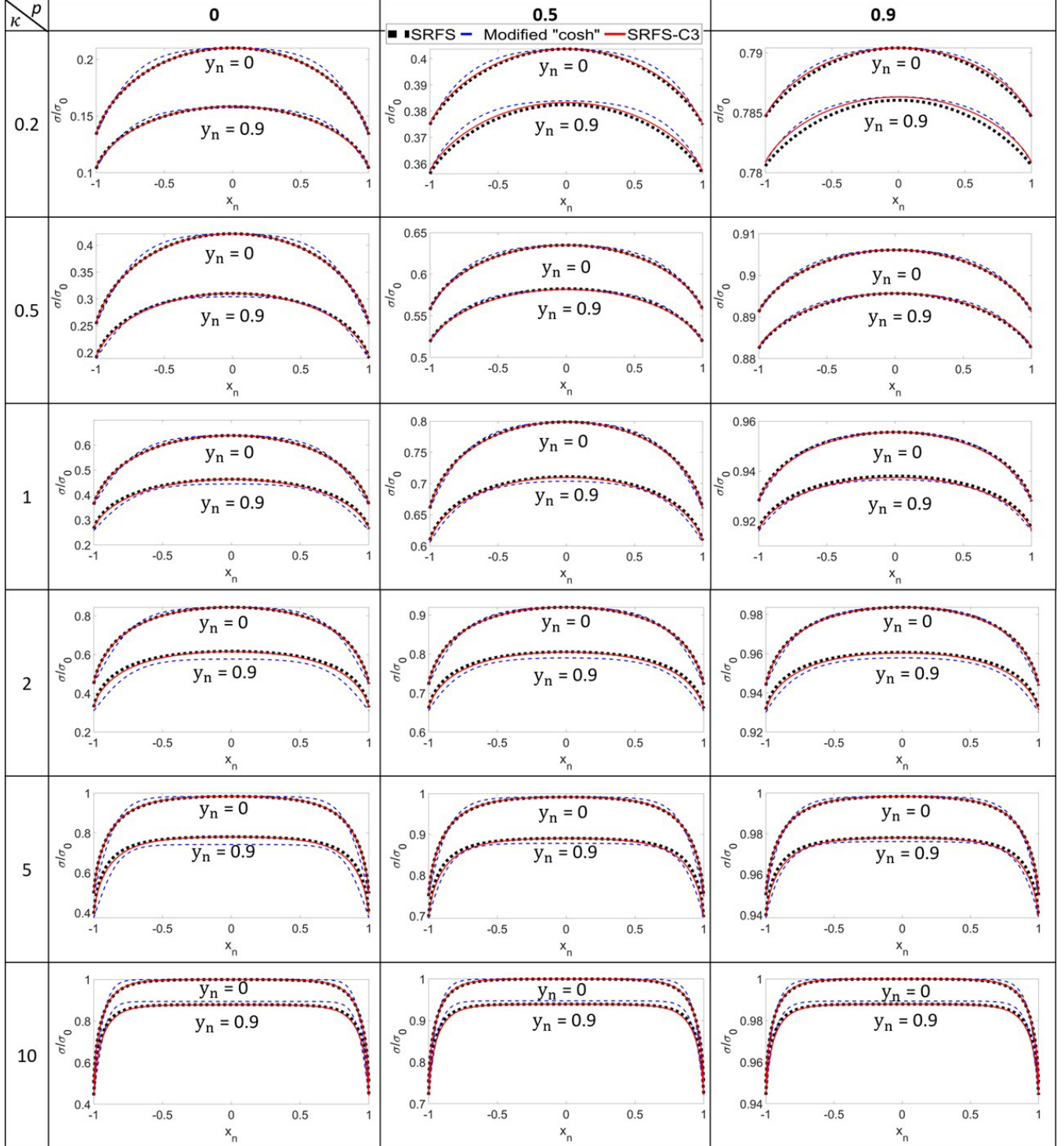


Fig. 4. The spatial profiles for  $\sigma/\sigma_0$  (conductivity normalized to bulk conductivity) versus  $x_n$  ( $x_n=x/(a/2)$ ) for  $y_n$  ( $y_n=y/(b/2)$ ) = 0, 0.9 for different  $\kappa$  and  $p$ . The model parameters correspond to the approximate fitting scenario.



> REPLACE THIS LINE WITH YOUR MANUSCRIPT ID NUMBER (DOUBLE-CLICK HERE TO EDIT) <

$$\sigma_{avg} = \sigma_{SRFS}(0,0) - (\sigma_{SRFS}(0,0) - \sigma_{SRFS}(1,0)) \times \left[ 1 - \frac{\sinh(\beta_a)}{\xi_1(\beta_a)} \right] - (\sigma_{SRFS}(0,0) - \sigma_{SRFS}(0,1)) \times \left[ 1 - \frac{\sinh(\beta_b)}{\xi_1(\beta_b)} \right] \\ - (\sigma_{SRFS}(0,1) + \sigma_{SRFS}(1,0) - \sigma_{SRFS}(0,0) - \sigma_{SRFS}(1,1)) \times \left[ 1 - \frac{\sinh(\beta_a)/\beta_a}{\xi_1(\beta_a)} \right] \times \left[ 1 - \frac{\sinh(\beta_b)/\beta_b}{\xi_1(\beta_b)} \right]$$

where

$$\xi_1(\beta_a) = 2 \times [\cosh(\beta_a)(Chi(2\beta_a) - Chi(\beta_a)) - \sinh(\beta_a)(Shi(2\beta_a) - Shi(\beta_a))] \\ \xi_1(\beta_b) = 2 \times [\cosh(\beta_b)(Chi(2\beta_b) - Chi(\beta_b)) - \sinh(\beta_b)(Shi(2\beta_b) - Shi(\beta_b))] \\ \kappa_a = \frac{a}{\lambda_0}, \kappa_b = \frac{b}{\lambda_0} \quad \beta_a = \frac{2}{\pi} \kappa_a + \tanh\left(\frac{\kappa_a}{1.2p}\right), \beta_b = \frac{2}{\pi} \kappa_b + \tanh\left(\frac{\kappa_b}{1.2p}\right) \quad (15)$$

approximate analytical expressions from [12] and obtain an accurate continuous model. The only downside compared to the analytical expressions in [12] is that the proposed model requires four values by computing the integrals in (1), which makes it semi-analytical.

To obtain the average conductivity of the interconnect ( $\sigma_{avg}$ ), we perform a double integral of (10) with respect to  $x_n$  and  $y_n$  (with integral limits of -1 to 1) and divide by the cross-sectional area to obtain (15).

We compare  $\sigma_{avg}$  with those obtained by numerically integrating the SRFS model and computing the average for different  $p$  and  $\kappa_a$  for square wires ( $\kappa_a = \kappa_b$ ). The comparison is illustrated in Fig. 5 showing a close match across different  $\kappa$  and  $p$  values between SRFS and SRFS-C3. We also compare the average conductivity obtained from SRFS-C3 i.e. (15) with the values from the models in [12] for  $p=0$  in Fig. 6, showing a close match.

Using the same approach as in the 2D case, we can obtain the average conductivity of the interconnect ( $\sigma_{avg}$ ) for thin film shown in (16).

$$\sigma_{avg} = \sigma_{SRFS}(0,0) \\ - (\sigma_{SRFS}(0,0) - \sigma_{SRFS}(0,1)) \times \left[ 1 - \frac{\sinh(\beta_b)}{\xi_1(\beta_b)} \right] \quad (16)$$

The comparison between the SRFS-C3 and SRFS model for thin films is shown in Fig.7 for two sets of  $p$  values  $p=0$  and  $p=0.5$ . Note for thin films, we set  $\kappa_a \rightarrow \infty$  and study the effect of different  $\kappa_b$ . Our SRFS-C3 model matches the results from the SRFS model for both  $p$  values and wide range of dimensions. We also compare the average conductivity from the proposed SRFS-C3 model with the original FS model [11] for a thin film in Fig.8, showing a good match, which validates the SRFS-C3 model and the semi-analytical expression in (15).

The proposed model in (15) offers a continuous analytical model for average conductivity accounting for surface scattering and providing relationships to physical parameters ( $p$ ,  $\lambda_0$ ,  $a$  and  $b$ ). It only requires four computations of complex integrals given by (1), but despite that, the computation is fast enough for incorporation in circuit simulators and compatible CAD software.

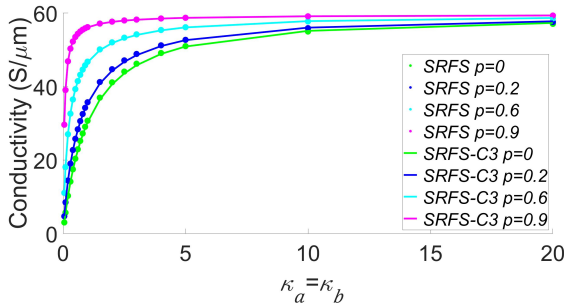


Fig. 5. SRFS model versus SRFS-C3 model for square wire with different  $\kappa$  and  $p$  showing a good match.

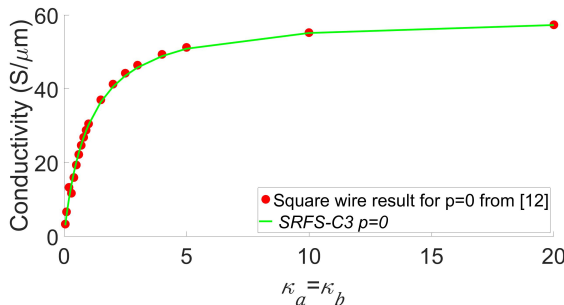


Fig. 6. Square wire SRFS-C3 model compared with 2D FS model from [12] for different  $\kappa$  and  $p$  showing a close match.

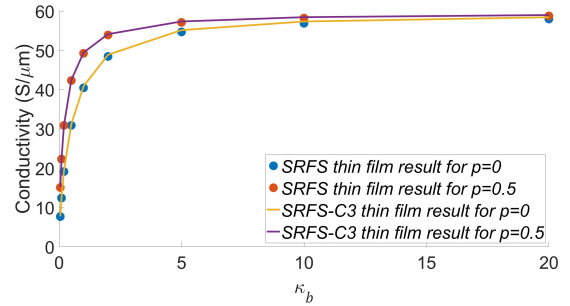


Fig. 7. Thin film SRFS-C3 model versus thin film SRFS for different  $\kappa$  and  $p$  showing a good match.

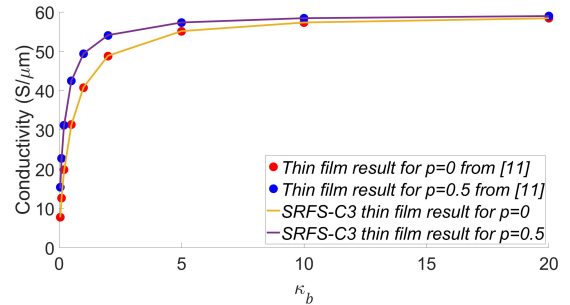


Fig. 8. Thin film SRFS-C3 model compared with thin film FS model from [11] for different  $\kappa$  and  $p$  showing a close match.

> REPLACE THIS LINE WITH YOUR MANUSCRIPT ID NUMBER (DOUBLE-CLICK HERE TO EDIT) <

It is noteworthy that if we try computing the average conductivity using the modified “cosh” model, it leads to complicated integrals, for which analytical expressions are challenging to obtain. This is because it is based on resistivity addition. Hence, we need to first take the reciprocal of (13) and then compute the double integral. On the contrary, with the proposed SRFS-C3 model, we are able to obtain a closed form expression for average conductivity.

Before we conclude, it is worth mentioning that it may be possible to augment the circuit-compatibility of our model by formulating approximate analytical expressions for  $\sigma_{SRFS}(0,0)$ ,  $\sigma_{SRFS}(1,0)$ ,  $\sigma_{SRFS}(0,1)$ ,  $\sigma_{SRFS}(1,1)$  as function of  $\kappa$  and  $p$ . Thus, by using the analytical model (instead of using the integral-based expressions of (1)) in conjunction with the SRFS-C3 approach, one can potentially speed up the computations at the cost of accuracy. This can be investigated in a future work.

## VII. CONCLUSION

We proposed a 2D spatially resolved FS based circuit compatible conductivity (SRFS-C3) model for rectangular interconnects. The proposed model uses an analytical function to predict the spatial profile by using only four conductivity values from the physical SRFS model (derived in Part I). This makes the SRFS-C3 model circuit compatible. Our model not only offers spatial resolution of conductivity (which matches closely with the physical SRFS model) but also accurately predicts the trends for a wide range of values for specularity, electron mean free path and interconnect dimensions. Additionally, we also obtain a continuous closed form expression for the average conductivity using the SRFS-C3 model, which is valid for a wide range of physical parameters and overcomes the limitations of previous models for average conductivity. We compare the SRFS-C3 model with a “cosh” based model [9] appropriately modified for a fair comparison. The key benefits of our approach include: (1) The proposed SRFS-C3 is based on conductivity subtraction which is more physical compared to resistivity addition that the modified “cosh” model uses. (2) The SRFS-C3 model is integrable to find the average conductivity, while the modified “cosh” model yields expressions that cannot be integrated. (3) The compact model for the fitting parameter of the SRFS-C3 model is more elegant and accurate. Overall, we find that the proposed SRFS-C3 model offers an excellent match to the SRFS model and is more accurate than the modified “cosh” model.

## ACKNOWLEDGMENT

This work was supported, in part, by SRC/NIST-funded NEWLIMITS Center (Award number 70NANB17H041)

## REFERENCES

- [1] A. P. Jacob, R. Xie, M. G. Sung, L. Liebmann, R. T. P. Lee, and B. Taylor, “Scaling Challenges for Advanced CMOS Devices,” *International Journal of High Speed Electronics and Systems*, p. 1740001, 2017, [Online]. Available: [www.worldscientific.com](http://www.worldscientific.com)
- [2] R. Brain, “Interconnect scaling: Challenges and opportunities,” in *2016 IEEE International Electron Devices Meeting (IEDM)*, 2016, pp. 9.3.1-9.3.4. doi: 10.1109/IEDM.2016.7838381.
- [3] X. Chen, C.-L. Lo, M. C. Johnson, Z. Chen, and S. K. Gupta, “Modeling and Circuit Analysis of Interconnects with TaS<sub>2</sub> Barrier/Liner,” in *2021*

- Device Research Conference (DRC)*, 2021, pp. 1–2. doi: 10.1109/DRC52342.2021.9467160.
- [4] C. L. Lo *et al.*, “Opportunities and challenges of 2D materials in back-end-of-line interconnect scaling,” *Journal of Applied Physics*, vol. 128, no. 8. American Institute of Physics Inc., Aug. 28, 2020. doi: 10.1063/5.0013737.
- [5] R. L. Graham *et al.*, “Resistivity dominated by surface scattering in sub-50 nm Cu wires,” *Appl Phys Lett*, vol. 96, no. 4, 2010, doi: 10.1063/1.3292022.
- [6] W. L. Wang *et al.*, “The Reliability Improvement of Cu Interconnection by the Control of Crystallized  $\alpha$ -Ta/TaN<sub>x</sub> Diffusion Barrier,” *J Nanomater*, vol. 2015, 2015, doi: 10.1155/2015/917935.
- [7] D. Edelstein *et al.*, “A high performance liner for copper damascene interconnects,” in *Proceedings of the IEEE 2001 International Interconnect Technology Conference (Cat. No.01EX461)*, 2001, pp. 9–11. doi: 10.1109/IITC.2001.930001.
- [8] E. H. SONDHEIMER, “Influence of a Magnetic Field on the Conductivity of Thin Metallic Films,” *Nature*, vol. 164, no. 4178, pp. 920–921, 1949, doi: 10.1038/164920a0.
- [9] I. Ciofi *et al.*, “Impact of Wire Geometry on Interconnect RC and Circuit Delay,” *IEEE Trans Electron Devices*, vol. 63, no. 6, pp. 2488–2496, Jun. 2016, doi: 10.1109/TED.2016.2554561.
- [10] T. Lu and A. Srivastava, “Detailed electrical and reliability study of tapered TSVs,” in *2013 IEEE International 3D Systems Integration Conference (3DIC)*, 2013, pp. 1–7. doi: 10.1109/3DIC.2013.6702350.
- [11] E. H. Sondheimer, “The mean free path of electrons in metals,” *Adv Phys*, vol. 1, no. 1, pp. 1–42, 1952, doi: 10.1080/00018735200101151.
- [12] D. K. C. Macdonald and K. Sarginson, “Size Effect Variation of the Electrical Conductivity of Metals,” 1950. [Online]. Available: <https://about.jstor.org/terms>